Research Square

Preprints are preliminary reports that have not undergone peer review.
They should not be considered conclusive, used to inform clinical practice,
or referenced by the media as validated information.

Mechanisms of Erbium Ion-Induced Mutagenesis and Xylanase Production Enhancement in Bacillus subtilis

Zhenyi Yao
Inner Mongolia University of Technology
Yunshu Xiao
Inner Mongolia University of Technology
Yongli Li
Inner Mongolia University of Technology
Jinna Cui
Inner Mongolia University of Technology
Zhanying Liu
Inner Mongolia University of Technology
jianhua hu
hhu79@imut.edu.cn

Inner Mongolia University of Technology

Research Article

Keywords: xylanase, Bacillus subtilis, various rare earth ions

Posted Date: November 17th, 2026

DOI: https://doi.org/10.21203/rs.3.rs-11587948/v1

License: This work is licensed under a Creative Commons Attribution 4.0 International License.
Read Full License

Additional Declarations: No competing interests reported.

Mechanisms of Erbium Ion-Induced Mutagenesis and Xylanase Production Enhancement in Bacillus subtilis

Zhenyi Yao[a,b,c], Yunshu Xiao[c], Yongli Li[a,b,c], Jinna Cui [a,b,c], Zhanying Liu [a,b,c], Jianhua Hu [a,b,c*]

[a] Inner Mongolia Key Laboratory of Synthetic Biology, Inner Mongolia University of Technology, Hohhot, 010051, Inner Mongolia, China

b Pilot-scale Capacity Construction Platform for Biomanufacturing of the Ministry of Industry and Information Technology, Hohhot, 010051, Inner Mongolia, China

c College of Chemical Engineering, Inner Mongolia University of Technology, Hohhot, 010051, Inner Mongolia, China

*Corresponding authors:

Jianhua Hu Tel: +86 15849384279, E-mail: jhhu79@imut.edu.cn

Abstract

Xylan, the second most abundant polysaccharide after cellulose, is a major component of plant cell walls. In this study, we investigated the effects of various rare earth ions at different concentrations on the growth and xylanase production of *Bacillus subtilis* 1.108 to breed high-xylanase-producing strains. The addition of rare earth ions during early fermentation significantly enhanced xylanase activity, and this enhancement was associated with genetic alterations rather than correlated with bacterial growth. To elucidate the underlying mechanism, we further characterized the mutated strain *B. subtilis* X-Er. Rare earth ion treatment induced notable changes in cell surface morphology and increased cell wall porosity, which may facilitate xylanase secretion. Additionally, modifications were observed in the xylanase gene sequence. Structural analysis of the xylanase enzyme revealed alterations in the active site, catalytic residues, secondary structure, and amino acid connectivity and arrangement. These cytomorphological and protein structural changes likely represent key factors contributing to enhanced enzyme activity. By focusing on the mutagenic effects of rare earth elements at the genetic level, this study provides mechanistic insights into the improved xylanase production in *Bacillus subtilis* 1.108 and offers valuable perspectives for understanding the biological effects of rare earth elements at the molecular level.

KEYWORD: xylanase; *Bacillus subtilis;* various rare earth ions

1. Introduction

The continuous growth in global energy demand, the depletion of crude oil reserves, and rising concerns about energy security have led to a shift in worldwide attention away from fossil fuels toward renewable energy sources, including lignocellulosic biomass[1, 2]. Lignocellulose is recognized as the most abundant renewable organic carbon resource on earth[3], and it is primarily composed of cellulose, hemicellulose, and lignin. The utilization of lignocellulose can be used to reduce environmental pollution caused by the use of fossil fuels, the recycling of agricultural ecosystems can be promoted[4, 5].Hemicellulose is mainly composed of xylanase. Xylanase can be employed by *Bacillus subtilis* as an auxiliary enzyme, and synergistic action with cellulase is used to degrade cellulose and enhance the efficiency of lignocellulosic biomass hydrolysis[6-8].

However, the xylanase production capacity of wild-type strains is generally low, thus limiting their direct application in industrial processes. Consequently, strain improvement has been a major focus to develop variants with high xylanase yields[9]. Conventional microbial breeding techniques encompass natural selection, mutagenesis, and hybridization. Among these, mutagenesis breeding allows for the rapid generation of large mutant libraries. By applying appropriate screening strategies, high-xylanase-producing strains can be isolated from these populations, resulting in significantly increasing microbial genetic diversity and economic potential[10]. Furthermore, Combined mutagenesis typically yields more significant results compared to single mutagenesis approaches[11, 12].

Rare earth ions (REIs), a unique class of metal ions, have recently been applied in the screening and breeding of high-yield microbial strains, with studies showing favorable experimental results and high genetic stability[13]. Accordingly, the roles of REIs in microbial metabolism, growth, and proliferation have been widely explored[14, 15]. Studies have demonstrated that REIs can induce hormesis in microorganisms, whereby low concentrations promote growth, whereas high

concentrations exhibit inhibitory effects[16]. Moreover, specific REIs treatments can significantly improve the physiological performance and enzyme production capacity of *B. subtilis*. For example, reported that Dy^{3+} and Nd^{3+} exerted mutagenic effects on the amylase gene of *B. subtilis*, leading to elevated amylase activity. Similarly, Kan found that treatment with appropriate concentrations of Nd^{3+} and Er^{3+} not only promoted the growth of *B. subtilis* but also enhanced the strain's resistance to ultraviolet radiation[17]. Collectively, these findings lay a foundation for understanding the regulatory effects of REIs on enzyme-related genes. Studies on broader microbial communities have also substantiated this concentration-dependent effect. Tang investigated the impact of lanthanum ions (La^{3+}) on soil microbial communities. Their results showed that when the soil adsorption capacity for La^{3+} ranged from 5% to 50%, bacterial growth was inhibited. Inhibition of actinomycetes and fungi occurred at adsorption capacities exceeding 30% and 50%, respectively[18]. In addition, a soil adsorption capacity above 10% resulted in a pronounced inhibition of soil ammonification. Beyond microbiology, REIs have been used as feed additives in animal husbandry to promote growth[19]. He reported that trace supplementation of REIs in broiler feed significantly increased growth performance and improved the feed conversion ratio by 3.4%[20]. In parallel, investigations into the genetic mechanisms underlying the effects of REIs have advanced.

In this study, rare earth elements were employed as additives to develop high-xylanase-producing strains of *B. subtilis*, thereby providing new microbial resources for xylanase-related applications. Furthermore, this work elucidates the mechanism by which rare earth elements enhance xylanase production in *B. subtilis*, offering valuable insights for future research on the application of rare earth elements in microbiology.

2. Materials and methods

2.1 Strains and medium

B. subtilis 1.108 was obtained from the China General Microbiological Culture Collection Center (CGMCC) under accession number 1.108. The composition of the

media is shown in Table 1. All chemicals used in the preparation of the media were of analytical grade (Merck).

Table 1 Composition of the culture medium.

Component	Concentration
Tryptone	10 g/L
Yeast extract	50 g/L
Sodium chloride	10 g/L
Ampicillin	100 μg/mL
Erythromycin	100 μg/mL
Coarse xylanase	2.5 g/L

Cultures were grown in 50 mL of the prepared medium in 250-mL Erlenmeyer flasks at 30℃ with shaking at 180 rpm. The inoculum size was adjusted to 10% (v/v) of the total culture volume.

2.2 Experimental Design

2.2.1 Effects of Various Rare Earth Ions at Different Concentrations on Xylanase Production by *B. subtilis*.

A single colony of *B. subtilis* was inoculated into LB medium and cultured at 30℃ with shaking at 180 rpm for 12 h (until the exponential phase) to prepare the seed culture. Then, 5 mL of this seed culture was transferred into 50 mL of fermentation medium to standardize the initial optical density (OD_{600}). At the time of inoculation (0 h), rare earth ions (Er^{3+}, Nd^{3+}, Sm^{3+}, Tm^{3+}, Gd^{3+}, Tb^{3+}, Sc^{3+}, Pr^{3+}, Ho^{3+}, Y^{3+}, La^{3+}, Eu^{3+}, and Ce^{3+}) were added aseptically at 1% (v/v) ratio to the fermentation system containing 0.2 M phosphate buffer (pH 7.0). The final concentrations of the ions ranged from 1×10^{-6} to 1×10^{-4} M. The cultures were incubated at 30 ℃ with shaking at 180 rpm. A control group, without rare earth ions, was included, and all cultures were prepared in triplicate.

2.2.2 Effects of Rare Earth Element Addition Time on the Growth and Xylanase Production of *B. subtilis*.

The cultivation conditions were identical to those described in Section 2.2.1, with the exception of the timing of rare earth ion addition. Following inoculation with the seed culture, sterile rare earth ion solutions were added at various time points (Table 2). All other parameters, including temperature, shaking speed, and medium composition, remained constant.

Table 2 Rare earth ion addition time points and corresponding experimental groups.

Experimental group	Er1	Er2	Er3	Er4
Adding time (h)	0	6	12	24

2.3 Genetic stability test

The selected strain was streaked onto solid LB medium containing 0.25% (w/v) crude xylanase and incubated at 30 ℃ for 2–3 d. A single colony was picked and inoculated into 50 mL of fermentation medium and cultured at 30 °C with shaking at 180 rpm for 12–14 h. The strain was serially subcultured for eight generations under the same conditions. Xylanase activity was measured after each subculture to assess the genetic stability of the strain.

2.4 Observation methods for cell phenotype and cell wall

2.4.1 Observation methods for cell morphology.

A 5 mL aliquot of bacterial culture in the logarithmic growth phase was centrifuged at 3000 rpm for 3 min, and the supernatant was discarded. The cell pellet was washed three times with phosphate buffer (pH 7.0) and then fixed with 2.5% (v/v) glutaraldehyde in the same buffer for 4 h at 4 °C. After fixation, the sample was centrifuged at 8000 rpm for 5 min, and the bacterial cells were subjected to graded dehydration using an ethanol series (30%, 50%, 70%, 80%, 90%, and 100%) with each step lasting 15–20 min. The dehydrated sample was then treated with a 1:1(v/v) mixture of ethanol and tert-butanol for 20 min, followed by two additional exchanges with pure tert-butanol (20 min each). Note that the tert-butanol substitution steps were performed at room temperature to maintain the solvent in a liquid state. Finally, the sample was lyophilized, sputter-coated with gold, and observed using scanning electron microscopy

(SEM) to examine cell morphology.

2.4.2 Methods for observing cell walls

A 5 mL aliquot of bacterial culture at the logarithmic growth phase was centrifuged at 8000 rpm for 5 min at 4℃. The pellet was washed repeatedly with sterile physiological saline. The cells were resuspended in 0.2 M phosphate buffer (pH 7.0) and disrupted by sonication on ice for 30 min at 100 W. The lysate was centrifuged at 1000 rpm for 10 min to remove insoluble debris, and the supernatant was collected. This supernatant was then centrifuged at 12,000 rpm for 20 min at 4℃. The resulting pellet was washed again with sterile physiological saline, centrifuged at 10,000 rpm for 10 min, and lyophilized to obtain the crude cell wall fraction.

For purification, the crude cell wall preparation was resuspended in phosphate buffer (pH 7.0). The suspension was treated with 50μL of deoxyribonuclease I (DNase I) solution (0.25% w/v in phosphate buffer, pH 7.0) at 37℃ for 1 h. Subsequently, 50μL of trypsin solution (0.25% w/v in phosphate buffer, pH 7.0) was added, and the mixture was incubated at 37℃ for an additional 2 h. Following enzymatic treatment, the sample was centrifuged at 1,000 rpm for 10 min at 4 ℃ to remove undigested debris, and the supernatant containing cell wall fragments was collected. This supernatant was then centrifuged at 12,000 rpm for 20 min at 4 ℃ to harvest the purified cell walls. The resulting pellet was washed three times with sterile distilled water (centrifugation at 12,000 rpm for 10 min between washes) and lyophilized. Finally, the dried powder was mounted on aluminum stubs, sputter-coated with gold, and examined using scanning electron microscopy (SEM) to characterize the cell wall morphology.

2.5 Cloning of xylanase gene

2.5.1 extraction of genomic DNA.

Genomic DNA was extracted from both *B. subtilis* 1.108 and *B. subtilis* X-Er, and DNA integrity was verified using agarose gel electrophoresis.

2.5.2 primer design.

The nucleotide sequences of the xylanase genes xynA (NCBI Gene ID: 939861), xynC (NCBI Gene ID: 937052), and xynD (NCBI Gene ID: 936433) from the reference strain *B. subtilis* 168 were retrieved from the NCBI GenBank database. Primers targeting these genes were designed using DNAMAN software and are listed in Table 3.

Table 3 Primers used for xylanase gene amplification.

Xylanase gene	Primer sequences
xynA	upstream primer：CCGGCGGGATCCATGTTTAAGTTTAAAAAG downstream primer：GGCCGCGGTTACCACACTGTTACGTTAG
xynC	upstream primer：CCGGATCCATGATTCCACGCATAAAAA downstream primer：GGCCGCGGTTAACGATTTACAACAAATG
xynD	upstream primer：GCGGATCCATGAGGAAAAAGTGTAGCGT downstream primer：GCCGCGGCTATCTTTGCGTAAACTG

2.5.3 The xylanase gene fragment was amplified by PCR.

PCR amplification was performed using Takara Ex Taq DNA polymerase. The genomic DNA of *B. subtilis* 1.108 and *B. subtilis* X-Er served as templates, using the primers listed in Table 3. The reaction mixture components are detailed in Table 4. The thermal cycling conditions were as follows: an initial denaturation at 95℃ for 10 s; followed by 30 cycles of denaturation at 95 ℃ for 10 s, annealing at 50 ℃ for 30 s, and extension at 72 °C for 2 min; a final extension was performed at 72 °C for 5 min.

Table 4. PCR reaction system.

PCR reaction system	Volume（μL）
DNA template	1
Upstream primer	0.5
Downstream primer	0.5
Ex-Taq DNA polymerase	0.5
dNTPs	2
10×Ex-Taq buffer	2.5
ddH_2O	18
Total volume	25

2.6 Comparing the changes of xylanase gene sequence before and after rare earth treatment.

The xylanase genes xynA and xynD from both the original *B. subtilis* 1.108 and the resulting mutant strain (designated *B. subtilis* X-Er) with enhanced xylanase production following rare-earth ion mutagenesis were sent to Sangon Biotech (Shanghai) for bidirectional sequencing. Raw sequencing data were processed, and the obtained target gene sequences were aligned for comparative analysis.

2.7 Comparing the structural changes of xylanase proteins structure before and after rare earth treatment.

The relative molecular masses and theoretical isoelectric points of the xylanase enzymes were predicted using DNAMAN compared between the original and mutant strains. Furthermore, the active sites, secondary structures, and three-dimensional models of the xylanase enzymes encoded by xynA and xynD from both the original and mutant *B. subtilis* strains were predicted using PROSITE, SOPMA, and EzMol, respectively, to evaluate structural differences.

Availability of data and materials

All data supporting the findings of this study are available within the paper and its supplementary materials.

3 Results and discussion

3.1 Effects of Rare Earth Ion Concentration on the Growth and Xylanase Production in *B. subtilis*.

3.1.1Effects of Rare Earth Ions on Growth and Xylanase Production in *B. subtilis*

Among the rare earth ions evaluated, Er^{3+} exhibited the strongest stimulatory effect on xylanase production in *B subtilis*, followed by Nd^{3+}, Sm^{3+}, Tm^{3+}, and Gd^{3+}, whereas Sc^{3+} showed the most pronounced inhibitory effect. As shown in Fig. 1, the addition of 1×10^{-4} M Er^{3+} resulted in the highest xylanase activity (133.79 U/mL), representing a 10.48% increase compared to the control strain *B. subtilis* 1.108 ($p < 0.01$). At the same concentration, Nd^{3+}, Sm^{3+}, Tm^{3+}, and Gd^{3+} increased enzyme activity by 9.38%, 8.74%, 6.08%, and 5.32%, respectively. In contrast, the addition of Sc^{3+} at 1×10^{-4} M reduced xylanase activity to 109.76 U/mL, representing a 9.33% decrease relative to the control strain.

These results indicate that while different rare earth ions and their concentrations differentially modulate the growth of *B. subtilis*, the relationship between bacterial growth and xylanase production is not strictly correlated. Specifically, rare earth ions that promoted growth did not invariably lead to increased enzyme activity, and conversely, those that inhibited growth did not always result in decreased enzyme production. This observation aligns with findings reported by Lu et al. who investigated the effects of La^{3+} on xylanase production in Penicillium verruculosum. Their study revealed that La^{3+} at 10^{-8} g/L increased xylanase activity by 68.3% compared to the untreated control, whereas at 10^{-1} g/L, it exhibited the strongest inhibitory effect, reducing activity by 72.3%. Therefore, in *B. subtilis* 1.108, xylanase biosynthesis appears to be dissociated from cellular growth, a phenomenon further supported by prior

research[22].

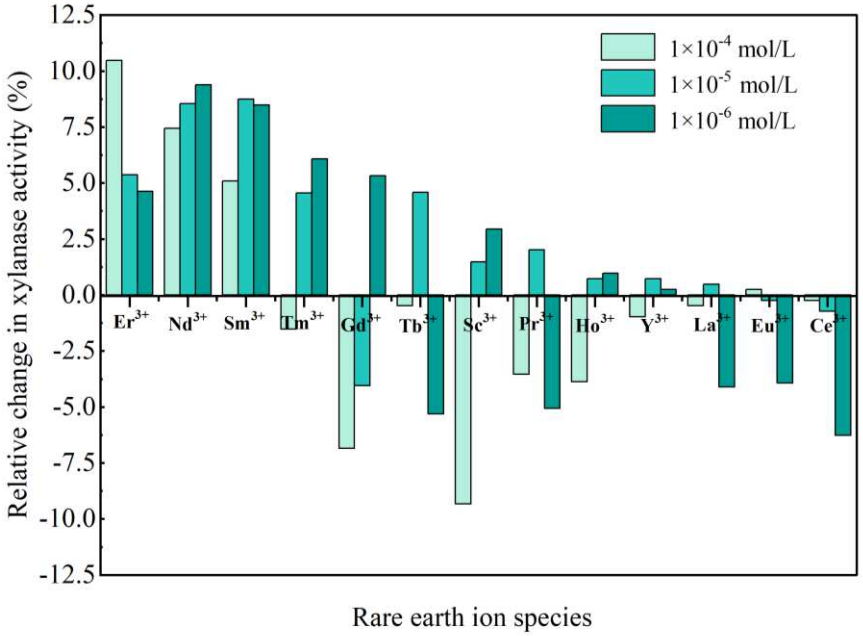


Fig.1 Effects of rare earth ion species and concentrations on xylanase production by *B. subtilis* 1.108.

3.1.2 Effects of addition time on the growth of *B. subtilis* and the production of xylanase

Based on the experimental results described above, the strain designated *B. subtilis* X-Er was supplemented with 1×10^{-4} M Er^{3+} at four distinct time points: 0, 6, 12, and 24 h post-inoculation. As summarized in Table 5, adding Er^{3+} at 0 h or 6 h yielded the highest xylanase activity (130.05 U/mL), representing a 9.8% increase over the control ($p < 0.01$). In contrast, the enzyme activity showed no significant improvement when the ions were added at 12 h or 24 h. As shown in Fig. 2, the addition of Er^{3+} at 0 h or 6 h resulted in faster bacterial growth and higher enzyme activity. A possible explanation is that early addition of Er^{3+} during cultivation enhanced xylanase production, thereby increasing enzymatic activity. When added at 12 h, although bacterial growth was stimulated, no significant improvement in enzyme activity was observed. Supplementation at 24 h had little effect on either growth or xylanase activity.

These results suggest that the optimal addition time for Er^{3+} ions is at 0 h or 6 h of cultivation, as this timing most effectively promoted xylanase production in *B. subtilis*.

Table 5 Effect of rare earth ion addition time on xylanase production by *B. subtilis* 1.108.

Addition time (h)	Enzyme activity (U/mL)	Increase rate (%)
control	118.44 ± 0.83^{Bb}	——
0	130.05 ± 2.09^{Aa}	9.80
6	130.05 ± 1.25^{Aa}	9.80
12	120.67 ± 5.36^{ABb}	1.88
24	118.95 ± 3.76^{Bb}	0.43

3.2 Effects of rare earth treatment on genetic stability.

As illustrated in Fig. 2, xylanase activity in *B. subtilis* X-Er remained stable at approximately 133 U/mL across all successive subcultures, with no statistically significant differences observed. These findings demonstrate that the *B. subtilis* X-Er strain possesses robust genetic stability

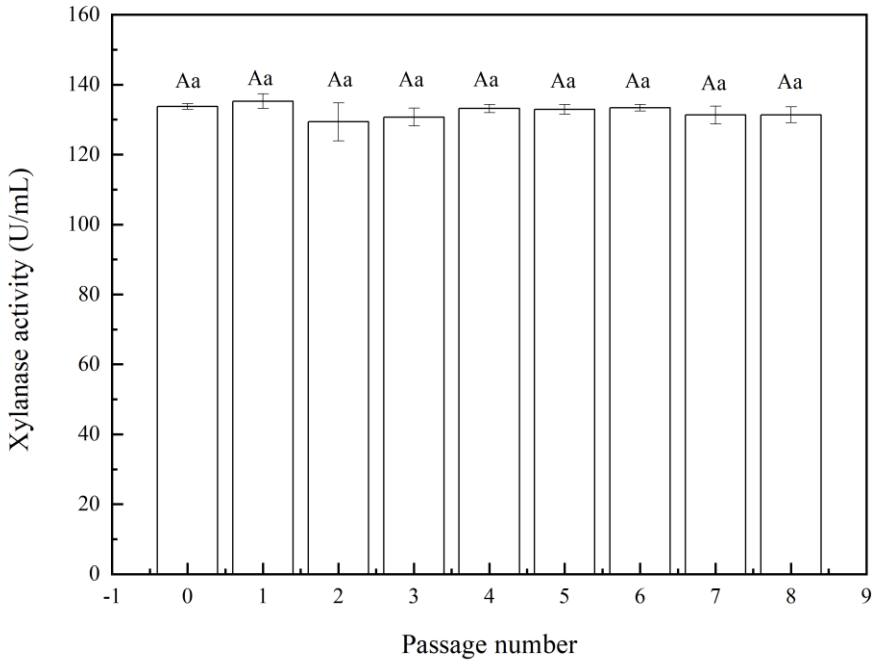
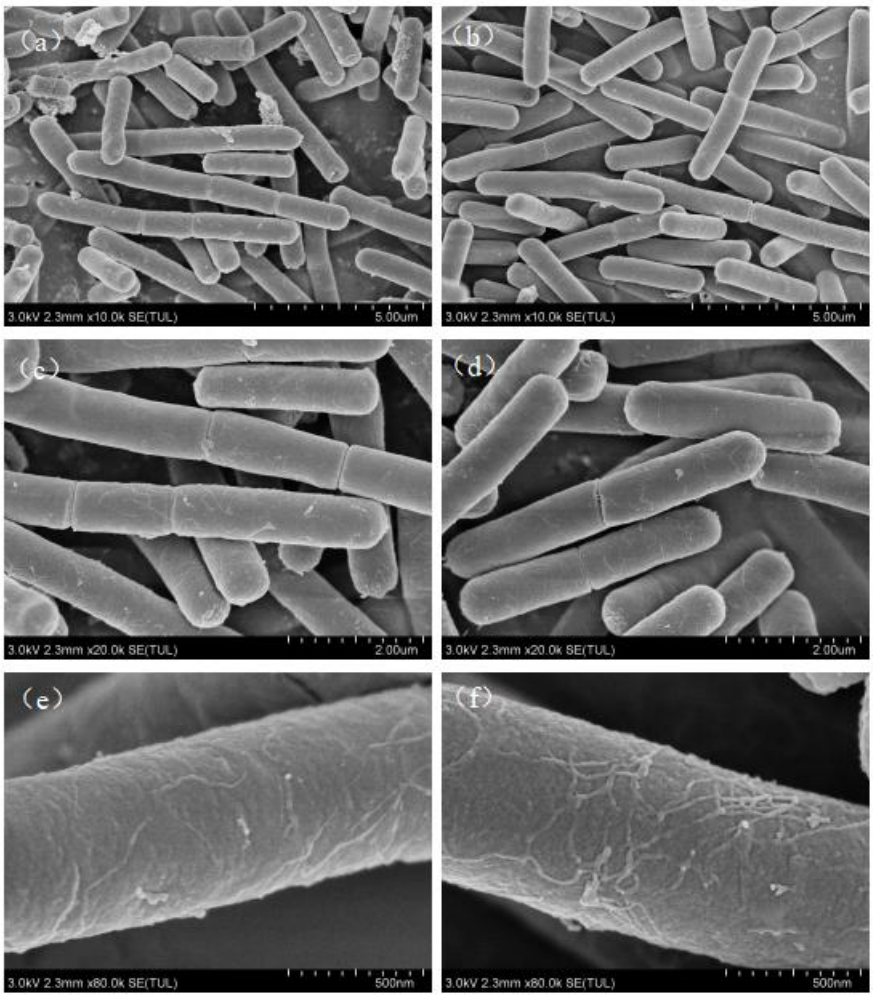


Fig 2 Genetic stability of *B subtilis X-Er.*

3.3 Results and Mechanistic Analysis

3.3.1 Effects of Rare Earth Elements on Cellular Phenotype of the Strain.

As shown in Fig 3 at magnifications of 10,000×, 20,000×, and 80,000×, the bacterial cells maintained a cylindrical rod-shaped morphology both before and after rare earth treatment, with no significant change in size. However, at the higher magnification (80,000×), the cell surface of the rare earth-treated strain appeared noticeably rougher than that of the untreated control. These results indicate that rare earth ions altered the surface characteristics of the cells without affecting their overall morphology.



（a）*B. subtilis* 1.108（×10000）；（b）*B. subtilis* X-Er（×10000）；

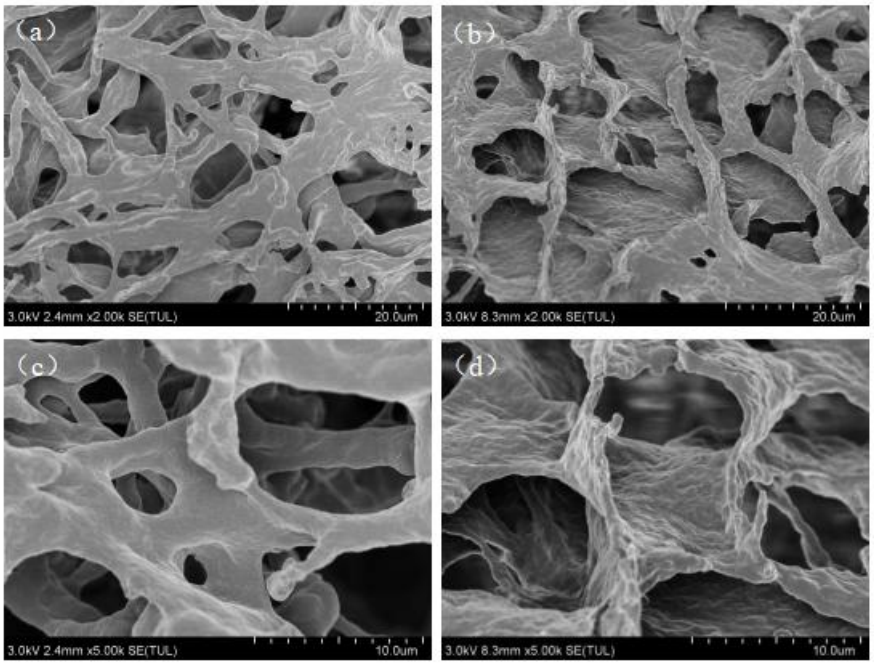
（c）*B. subtilis* 1.108（×20000）；（d）*B. subtilis* X-Er（×20000）；

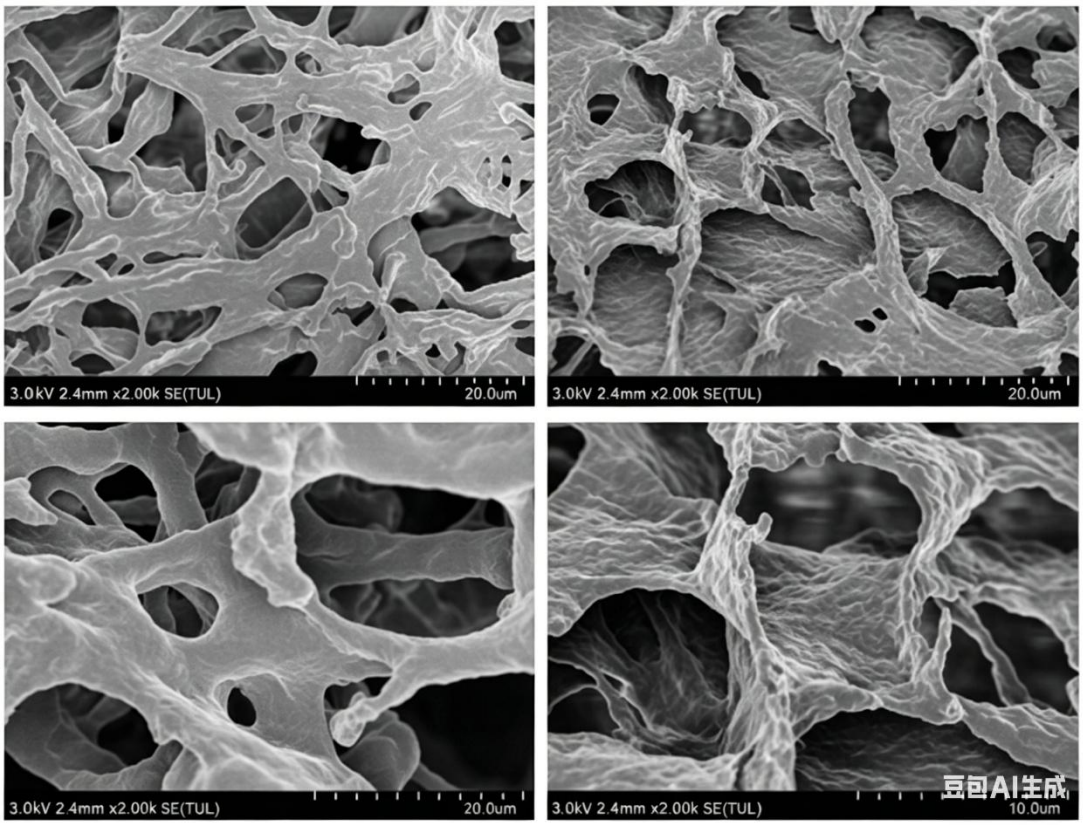
（e）*B. subtilis* 1.108（×80000）；（f）*B. subtilis* X-Er（×80000）；

Fig 3 Scanning electron miscroscope of *B. subtilis.*

3.3.2 Effects of rare earth elements on the cell wall of the strain.

As shown in Fig. 4, both before and after rare earth treatment, cell wall perforations were observed in the strains. However, following the treatment, the perforations appeared larger overall. This suggests that rare earth elements may have altered the cell wall structure of *B. subtilis*, leading to increased permeability. Such alterations likely facilitated the extracellular secretion of xylanase, thereby contributing to the enhanced xylanase production observed. Together this mechanism may contribute to the improved xylanase activity observed in the high-yielding strain in this study.





（a）*B. subtilis* 1.108（×2000）；（b）*B. subtilis* X-Er（×2000）；

（c）*B. subtilis* 1.108（×5000）；（d）*B. subtilis* X-Er（×5000）；

Fig 4 Scanning electron miscroscope of cell wal.l

3.3.3 genomic DNA extraction

As shown in Fig. 5, the extracted genomic DNA exhibited clear bands with sizes consistent with theoretical expectations, indicating its suitability for subsequent experimental procedures.

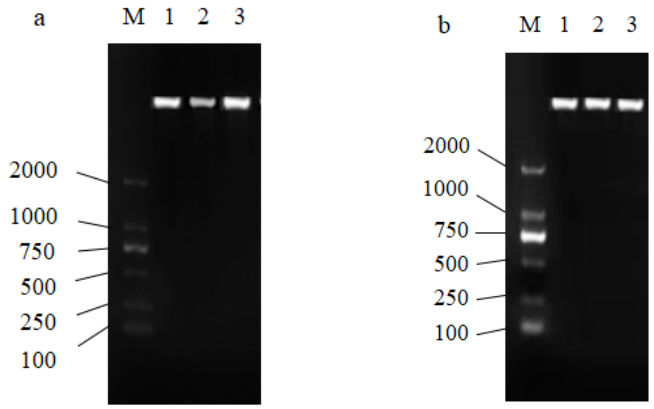


Fig.5 DNA electrophoresis figure of whole genome

3.3.4 Amplification of xylanase gene fragment

As shown in Fig. 6, the fragments of the xynA and xynD genes amplified using the complete genomes of *B. subtilis* 1.108 and *B. subtilis* X-Er as templates were relatively clear, and the band sizes were accurate.

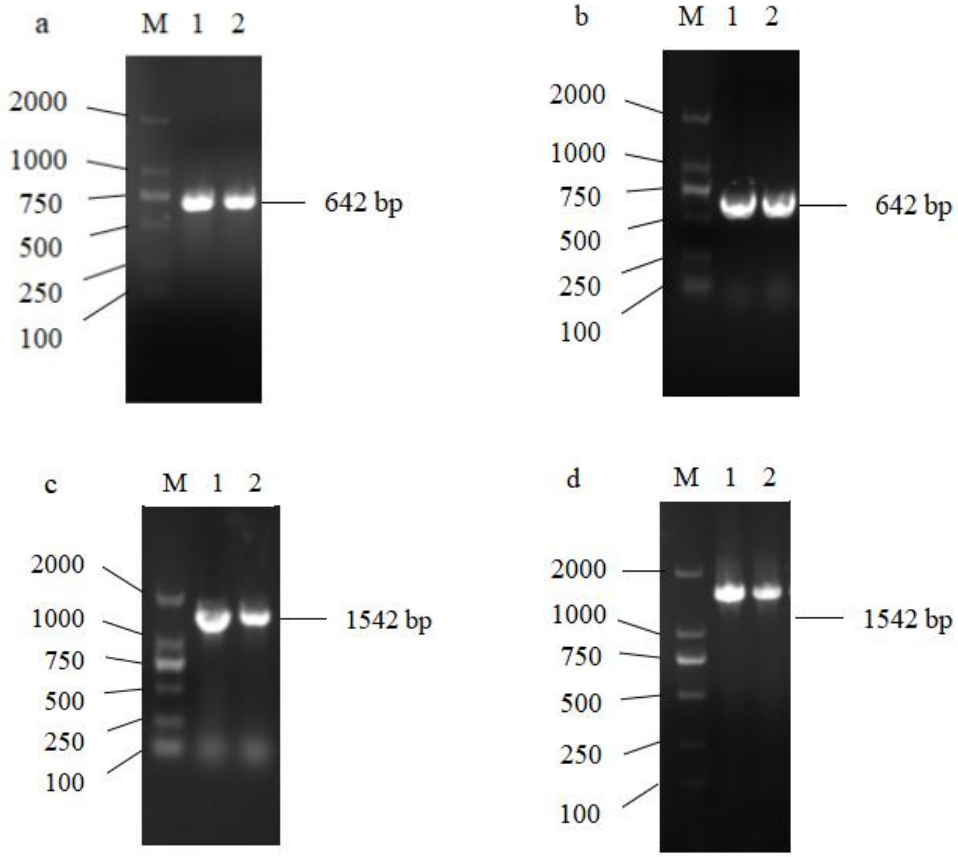


Fig 6 Target gene amplification result.

3.3.5 Changes of xylanase gene sequence

A comparative analysis of the xylanase gene sequences xynA and xynD from *B. subtilis* 1.108 and *B. subtilis* X-Er is shown in Fig. 3-6, and 3-7. Following rare earth treatment, mutations were observed in both xynA and xynD, primarily as substitution or insertion mutations. Specifically, only a single insertion mutation was detected in xynD. These results indicate that the addition of Er^{3+} ions altered the DNA sequences of the xylanase genes xynA and xynD. It can be inferred that these genetic changes led to structural

modifications in the corresponding enzymes, which subsequently contributed to enhanced xylanase activity.

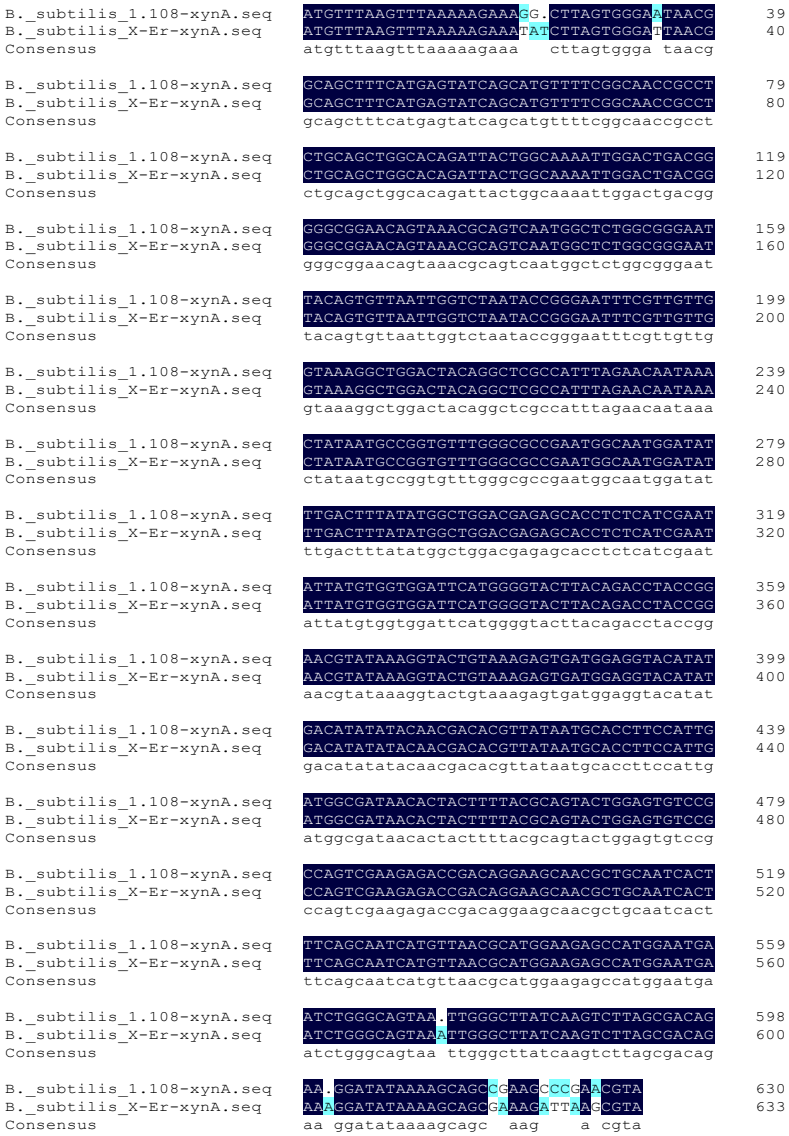


Fig 7 Comparison results of xynA gene sequence between *B. subtilis* 1.108 and *B. subtilis* X-Er.

```
B._subtilis_1.108-xynD.seq    ATGCGCCGCTTACCGCAGTTTCTATTTCTCTCCAGGATTG    40
B._subtilis_X-Er-xynD.seq     ATGCGCCGCTTACCGCAGTTTCTATTTCTCTCCAGGATTG    40
Consensus                     atgcgccgcttaccgcagtttctatttctctccaggattg

B._subtilis_1.108-xynD.seq    CGTTCCGCCTGTCGAAGGGACATTCAAGGTTCCGACAAGC    80
B._subtilis_X-Er-xynD.seq     CGTTCCGCCTGTCGAAGGGACATTCAAGGTTCCGACAAGC    80
Consensus                     cgttccgcctgtcgaagggacattcaaggttccgacaagc

B._subtilis_1.108-xynD.seq    TTACCGTTTGCACTGTCTAGCCGCACTTCTATTTTTCCGC    120
B._subtilis_X-Er-xynD.seq     TTACCGTTTGCACTGTCTAGCCGCACTTCTATTTTTCCGC    120
Consensus                     ttaccgtttgcactgtctagccgcacttctatttttccgc

B._subtilis_1.108-xynD.seq    CAAGAGCGGACGCTACATTTGCTTTGAACGTCTTGGCACC    160
B._subtilis_X-Er-xynD.seq     CAAGAGCGGACGCTACATTTGCTTTGAACGTCTTGGCACC    160
Consensus                     caagagcggacgctacatttgctttgaacgtcttggcacc

B._subtilis_1.108-xynD.seq    GCCTGACCCGAAGTCTGCATTTCCAACAGCAATCCAGTCT    200
B._subtilis_X-Er-xynD.seq     GCCTGACCCGAAGTCTGCATTTCCAACAGCAATCCAGTCT    200
Consensus                     gcctgacccgaagtctgcatttccaacagcaatccagtct

B._subtilis_1.108-xynD.seq    CCGTTATGAATGTTTGTGACATGTTGATTATTGACCGGCC    240
B._subtilis_X-Er-xynD.seq     CCGTTATGAATGTTTGTGACATGTTGATTATTGACCGGCC    240
Consensus                     ccgttatgaatgtttgtgacatgttgattattgaccggcc

B._subtilis_1.108-xynD.seq    CGCCGGGTGCTGAGGATGCCTCTGTCAAAATCCGTCCGTT    280
B._subtilis_X-Er-xynD.seq     CGCCGGGTGCTGAGGATGCCTCTGTCAAAATCCGTCCGTT    280
Consensus                     cgccgggtgctgaggatgcctctgtcaaaatccgtccgtt

B._subtilis_1.108-xynD.seq    CCAGGCAAACGTTTCCGCTTCTACCCGGTGATACGGATTC    320
B._subtilis_X-Er-xynD.seq     CCAGGCAAACGTTTCCGCTTCTACCCGGTGATACGGATTC    320
Consensus                     ccaggcaaacgtttccgcttctacccggtgatacggattc

B._subtilis_1.108-xynD.seq    AAGTTGGACAGCTGTTTGACACCTGCAAAATTTGCCGCTA    360
B._subtilis_X-Er-xynD.seq     AAGTTGGACAGCTGTTTGACACCTGCAAAATTTGCCGCTA    360
Consensus                     aagttggacagctgtttgacacctgcaaaatttgccgcta

B._subtilis_1.108-xynD.seq    CCTCTTGCAGGGAGCCATCTGGATTATGCACAAGCTTATT    400
B._subtilis_X-Er-xynD.seq     CCTCTTGCAGGGAGCCATCTGGATTATGCACAAGCTTATT    400
Consensus                     cctcttgcagggagccatctggattatgcacaagcttatt

B._subtilis_1.108-xynD.seq    AATATGGGGAGAACGGTATCCTTTGCCGGCCCCGTAAAGA    440
B._subtilis_X-Er-xynD.seq     AATATGGGGAGAACGGTATCCTTTGCCGGCCCCGTAAAGA    440
Consensus                     aatatggggagaacggtatcctttgccggccccgtaaaga

B._subtilis_1.108-xynD.seq    GCGGAGCTGACAGTTTGAGTATGATACACCACATACCACT    480
B._subtilis_X-Er-xynD.seq     GCGGAGCTGACAGTTTGAGTATGATACACCACATACCACT    480
Consensus                     gcggagctgacagtttgagtatgatacaccacataccact

B._subtilis_1.108-xynD.seq    CGTTTTTAAAATTGAAAACAGCATGGTGATTGTTCCCGCC    520
B._subtilis_X-Er-xynD.seq     CGTTTTTAAAATTGAAAACAGCATGGTGATTGTTCCCGCC    520
Consensus                     cgttttaaaattgaaaacagcatggtgattgttcccgcc

B._subtilis_1.108-xynD.seq    GCCTCCGAAAAATGCTCCCGGATTTTTCAGAAAGTGCCCT    560
B._subtilis_X-Er-xynD.seq     GCCTCCGAAAAATGCTCCCGGATTTTTCAGAAAGTGCCCT    560
Consensus                     gcctccgaaaaatgctcccggatttttcagaaagtgccct

B._subtilis_1.108-xynD.seq    CTATACGAAAAAGAATCCATAGGACTTGAGCTGGTCATAT    600
B._subtilis_X-Er-xynD.seq     CTATACGAAAAAGAATCCATAGGACTTGAGCTGGTCATAT    600
Consensus                     ctatacgaaaaagaatccataggacttgagctggtcatat

B._subtilis_1.108-xynD.seq    AGCCGATCTCACCTGGAGGTTTATCGGCCGGGTGAGCGCC    640
B._subtilis_X-Er-xynD.seq     AGCCGATCTCACCTGGAGGTTTATCGGCCGGGTGAGCGCC    640
Consensus                     agccgatctcacctggaggtttatcggccgggtgagcgcc

B._subtilis_1.108-xynD.seq    CCCGAAATTGATACAATAGGAATAGTAATATTTT.CCGTT    679
B._subtilis_X-Er-xynD.seq     CCCGAAATTGATACAATAGGAATAGTAATATTTTTCCGTT    680
Consensus                     cccgaaattgatacaataggaatagtaatatttt ccgtt

B._subtilis_1.108-xynD.seq    ATACTTATGCATTCCCGAATCTTCAAACATAAAAGGCGCA    719
B._subtilis_X-Er-xynD.seq     ATACTTATGCATTCCCGAATCTTCAAACATAAAAGGCGCA    720
Consensus                     atacttatgcattcccgaatcttcaaacataaaaggcgca

B._subtilis_1.108-xynD.seq    TCAATGGTCGATGCACTTCCGGCGACACTGGTCATATCAG    759
B._subtilis_X-Er-xynD.seq     TCAATGGTCGATGCACTTCCGGCGACACTGGTCATATCAG    760
Consensus                     tcaatggtcgatgcacttccggcgacactggtcatatcag
```

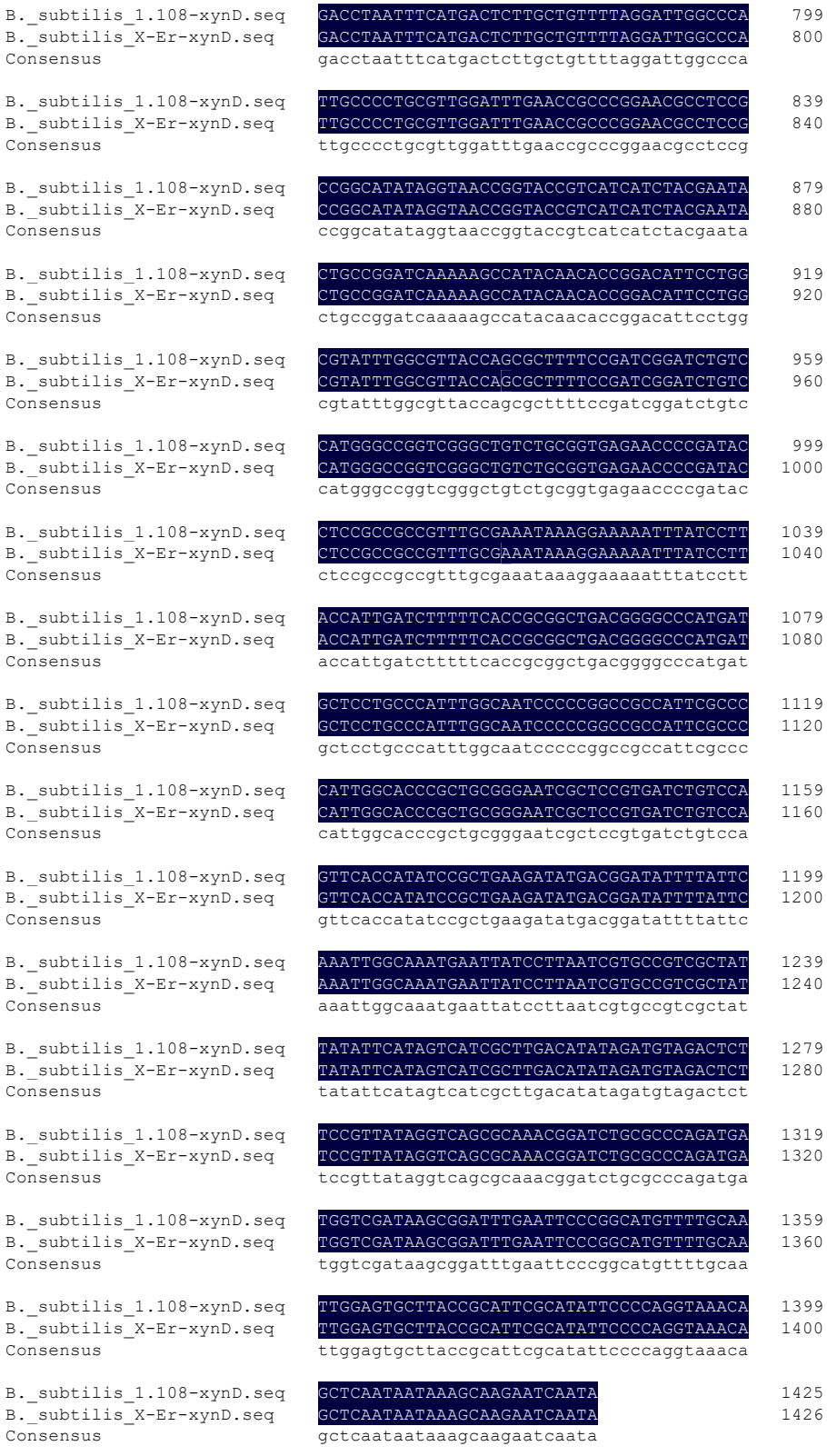
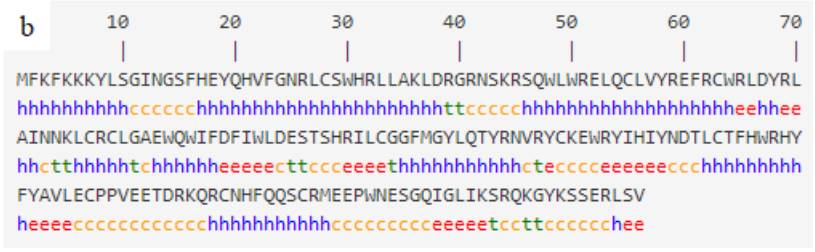


Fig 8 Comparison results of xynD gene sequence between *B. subtilis* 1.108 and *B. subtilis* X-Er.

3.3.6 Prediction of protein structure changes in xylanase

Using software (Section 2.7) for prediction, it was found that although rare earth treatment did not significantly alter the molecular weight or isoelectric point of *B. subtilis* xylanases XynA (210 → 196 aa, 22.90 → 24.18 kDa, pI 9.91 → 9.51) and XynD (457 → 456 aa, 54.94 → 50.53 kDa, pI 11.18 → 10.26), it resulted in the repositioning of the active site in XynA to position 8 and introduced new metal ion catalytic sites at positions 17 and 21, which significantly enhanced enzymatic activity. As shown in Fig. 10, the secondary structure of XynA shifted from being predominantly random coil to a structure rich in α-helices , with a notable increase in α-helix content and a decrease in β -sheets and random coils. In contrast, the secondary structures of xynD and the untreated xynA/xynD remained primarily composed of random coils.



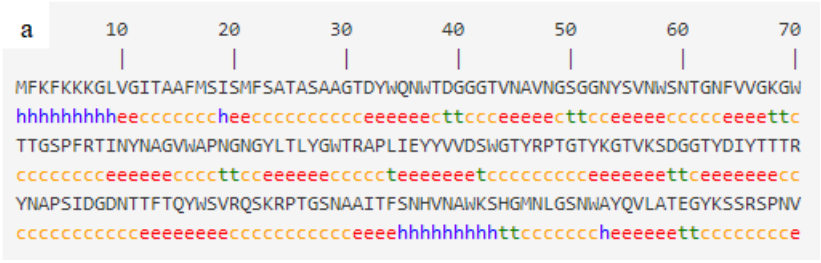






Fig 9 Prediction of protein secondary structure.

h: α-helix; e: β-sheet; t: β-turn; c: random coil

As shown in Fig. 11, rare earth ion treatment induced significant conformational rearrangements in the tertiary structures of *B. subtilis* xylanases xynA and xynD. These alterations manifested as distinct changes in spatial amino acid arrangement and fold topology, suggesting a modulation of their functional properties. Additionally major changes were also observed in the surface topography of enzymes, which may affect substrate binding. In summary, rare earth ions can modify the conformation of these xylanases, a key factor contributing to enhanced xylanase activity.

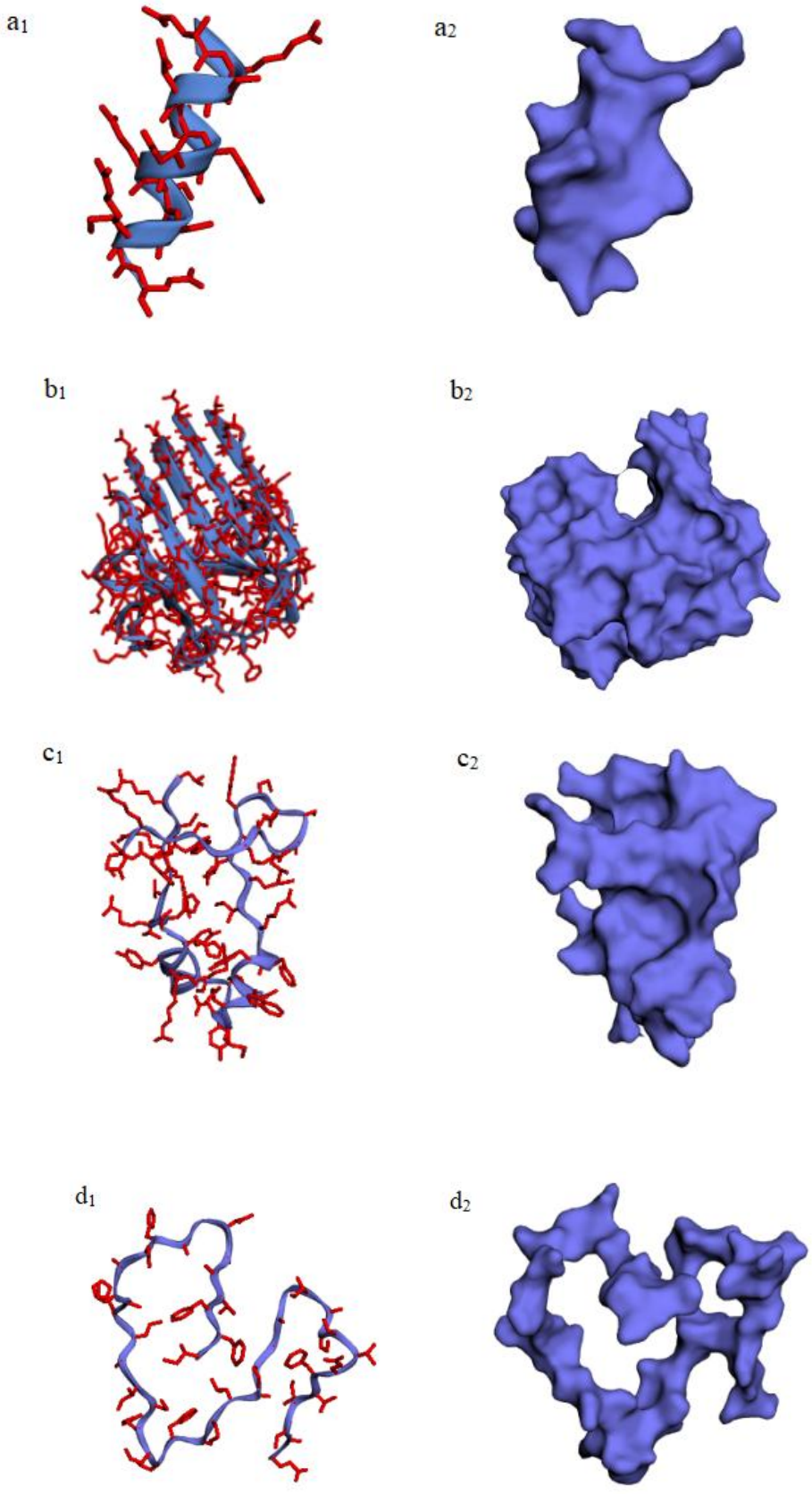


Fig 10 Protein tertiary structure prediction map.

Note : Figure a：*B. subtilis* 1.108-xynA；Figure b：*B. subtilis* X-Er-xynA；Figure c：*B. subtilis* 1.108-xynD；Figure d：*B. subtilis* X-Er-xynD。

4.Conclusions

Through a systematic investigation of rare earth ion species, concentrations, and addition timing on the growth and xylanase production of *B. subtilis* 1.108, we successfully isolated a mutant strain *B. subtilis* X-Er, characterized by enhanced genetic stability. Rare earth ions were found to either promote or inhibit xylanase production in *B. subtilis* to varying degrees. The addition of rare earth ions during the early fermentation phase (0–6 h) significantly enhanced xylanase activity. Interestingly, this increase in enzyme activity was not correlated with bacterial growth. To elucidate the mechanism by which rare earth ions enhance xylanase activity in *B. subtilis*, further analyses were conducted focusing on cellular phenotype, cell wall morphology, alterations, as well as changes in xylanase gene sequences and protein structure. The treated strain *B. subtilis* X-Er exhibited a rougher cell surface and increased cell wall porosity, leading to enhanced permeability and facilitating the secretion of xylanase into the extracellular environment. Moreover, rare earth treatment induced point mutations in the xylanase genes xynA and xynD. Although these mutations did not significantly alter the molecular mass or theoretical isoelectric point of the xylanase enzymes, they resulted in changes in active sites, catalytic residues, secondary structure composition, and the connectivity and arrangement of amino acids. These alterations led to substantial conformational changes in the protein structure.

This study not only presents a novel strategy for boosting xylanase yields in *B. subtilis* but also offers pivotal insights into the broader application of rare earth elements in microbial biotechnology.

Declarations

Ethics approval and consent to participate

Not applicable.

Consent for publication

Not applicable.

Competing interests

The authors declare that they have no competing interests.

Funding

This work was supported by grants from the Natural Science Foundation of Inner Mongolia (2025LHMS02009).

This work was supported by grants from the National Natural Science Foundation of China (22568032).

This work was supported by grant from the Special Project of the Innovation Consortium for Key Industrial Chains of Inner Mongolia Autonomous Region (2025ZDLH0006).

Reference

[1] Sulis B D, Lavoine N, Sederoff H, et al.Advances in lignocellulosic feedstocks for bioenergy and bioproducts[J].Nature Communications,2025,16(1):1244-1244.

[2] Deepak K, Kumar P S, Ki-Hyun K. Recent advances in metagenomic analysis of different ecological niches for enhanced biodegradation of recalcitrant lignocellulosic biomass[J].Environmental Research, 2022, 215(P2) :114369-114369.

[3] Jiju P S, Patel A K, Shruthy N S, et al. Sustainability through lignin valorization: recent innovations and applications drivingindustrial transformation[J]. Bioresources and Bioprocessing, 2025, 12(1): 88.

[4] S M S ,V D G .Lignocellulosic biomass: Hurdles and challenges in its valorization.[J].Applied microbiology and biotechnology,2019,103(23-24):9305-9320.

[5] Ao T J, Li D, et al. Valorizing Every Carbon Atom: A Cascade Bioprocess for Advanced Biofuels from Corn-Stover-Derived Lignocellulose[J]. Environmental Science & Technology, 2025, 59(49):21345-21354.

[6] Yu H, Li Y, Zhang L, et al. A multi-enzyme producing Bacillus subtilis YCXW-01: Isolation, genomic characterization, and potentials in tobacco stem degradation[J]. Frontiers in Microbiology, 2025, 16:1717865.

[7] Kumar A, Saini R. Consolidated biosaccharification of corn cob by novel lignocellulolytic enzymes from Bacillus subtilis CFB-09[J]. Biotechnology and Bioengineering, 2025, 122(4):1124-1136.

[8] Malik W A, Javed S. Biochemical characterization of cellulase from Bacillus subtilis strain and its effect on digestibility and structural modifications of lignocellulose-rich biomass[J]. Frontiers in Bioengineering and Biotechnology, 2021, 9:800265.

[9] Qinghui Y, Yuncheng L, Bo W, et al. Novel mutagenesis and screening technologies for food microorganisms: advances and prospects.[J]. Applied microbiology and biotechnology, 2020,104(4):1517-1531.

[10] Grid. C R I S, Grid. D O E H, Grid. D O C S, et al. LD 50 determination and phenotypic evaluation of three Echeveria varieties induced by chemical mutagens[J]. Toxicology and Environmental Health Sciences, 2020,12(1):1-9.

[11] Moritz H, Virginia K, Kira A, et al. Unbiased compound-protein interface mapping

and prediction of chemoresistance loci through forward genetics in haploid stem cells.[J]. Oncotarget, 2018,9(11):9838-9851.

[1] State Key Laboratory Of Food Science And Technology J U W J, et al. Insights into hydrolysis versus transfructosylation: Mutagenesis studies of a novel levansucrase from Brenneria sp. EniD312[J]. International Journal of Biological Macromolecules, 2018,116:335-345.

[2] Yunshu X, Wenzheng Y, Yongli L,etal. Study on the rare earth breeding of high-yield xylanase in Bacillus subtilis 1.108[J]Journal of Inner Mongolia University of Technology（Natural Science Edition）2024,43(03):224-228.

[3] VESTERGAARD M, HAQUE M F U, MARTÍNEZ-GÓMEZ N C. Changes in growth, lanthanide binding, and gene expression in Pseudomonas alloputida KT2440 in response to light and heavy lanthanides[J]. mSphere, 2024, 9(9):e00685-24.

[4] NISHIDA H, KATO J. Undecaprenyl pyrophosphate involvement in susceptibility of Bacillus subtilis to rare earth elements[J]. Journal of Bacteriology, 2012, 194(20):5528-5535.

[5] Furst A . Hormetic effects in pharmacology: pharmacological inversions as prototypes for hormesis.[J]. health physics, 1987, 52(5):527-30.

[6] Chungang K, Dongyan Z, Qingzhang H, et al. Study on the radiation resistance of Bacillus subtilis by Nd and Er[J]. Journal of Inner Mongolia University of Technology（Natural Science Edition, 2012(04):15-18.

[7] Lu Q, Gao Z, Wang L, et al. . Mechanism of La^{3+} effect on xylanase production by Penicillium citrinum. Chinese Rare Earths[J], 2020,41(1):78–84.

[8] Tang X, Zhang Z, Zhou B, etal. EffectofLanthanumonQuantityofMajorMicroorganismGroupsinYellowCinnamon Soil[J]. Journal of Rare Earths, 1998(03):34-38.

[9] He M L, Wehr U, Rambeck A. Rare earth elements-a new generation of growth promoters for pigs?[J]. Archives of Animal Nutrition,2000,53(4).